

# SpatialDreamer: Self-supervised Stereo Video Synthesis from Monocular Input

Zhen Lv, Yangqi Long, Congzhentao Huang, Cao Li, Chengfei Lv, Hao Ren, Dian Zheng  
Alibaba Group

## Abstract

*Stereo video synthesis from a monocular input is a demanding task in the fields of spatial computing and virtual reality. The main challenges of this task lie on the insufficiency of high-quality paired stereo videos for training and the difficulty of maintaining the spatio-temporal consistency between frames. Existing methods primarily address these issues by directly applying novel view synthesis (NVS) techniques to video, while facing limitations such as the inability to effectively represent dynamic scenes and the requirement for large amounts of training data. In this paper, we introduce a novel self-supervised stereo video synthesis paradigm via a video diffusion model, termed **SpatialDreamer**, which meets the challenges head-on. Firstly, to address the stereo video data insufficiency, we propose a **Depth based Video Generation module DVG**, which employs a forward-backward rendering mechanism to generate paired videos with geometric and temporal priors. Leveraging data generated by DVG, we propose **RefinerNet** along with a self-supervised synthetic framework designed to facilitate efficient and dedicated training. More importantly, we devise a consistency control module, which consists of a metric of stereo deviation strength and a **Temporal Interaction Learning module TIL** for geometric and temporal consistency assurance respectively. We evaluated the proposed method against various benchmark methods, with the results showcasing its superior performance.*

## 1. Introduction

Stereo video synthesis from a monocular input aims to generate the target-view video based on the given view with geometric and spatio-temporal consistency, which has a wide range of applications in 3D model reconstruction [6], 3D movie production [18, 38], and Apple Vision Pro (AVP) [42] like virtual reality content.

The primary difficulties of this task stem from the lack of adequate high-quality paired stereo videos for training, and the challenge of preserving the geometric consistency between two views as well as maintaining the temporal consistency across generated frames. Traditional methods for

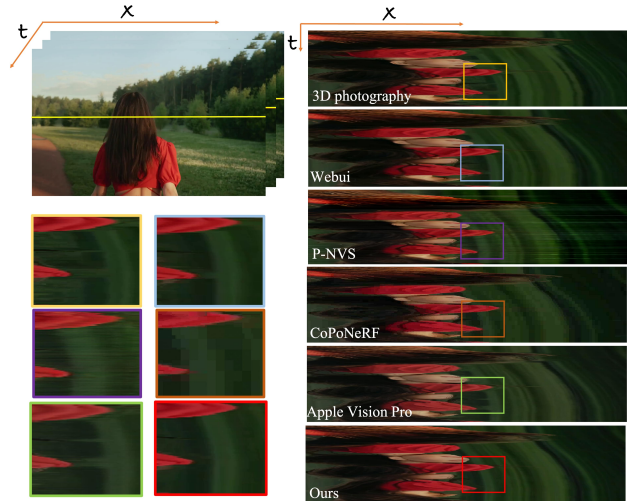


Figure 1. Visualization of the temporal consistency in stereo video generated by different methods. We extract the yellow line of each frame and stack them together. A good result should show a natural transition in the  $t$  dimension.

generating stereo content involve capturing scenes using dual-camera setups [50, 57, 68, 74]. However, the acquisition of these images involves the use of a professional-grade camera, resulting in substantial costs. Recent advancements in deep learning mainly handle these problems by directly applying single to stereo or multi-view image generation techniques to video, while often facing challenges related to geometric and spatio-temporal inconsistencies [21, 31, 39, 48, 64, 65]. As shown in Fig 1, methods based on NVS are challenging to maintain accurate spatio-temporal consistency, and even the recently released AVP 3D photo converter [2] may inevitably result in content flickering and inconsistency when applied to video synthesis. This is due to the difficulty of handling the temporal coherence between frames and the spatial information between paired views in complex dynamic scenes.

In this paper, we propose a self-supervised stereo video synthesis paradigm via a video diffusion model, termed SpatialDreamer, which will meet the data insufficiency and spatio-temporal inconsistency at once. Two novel designs

make our SpatialDreamer non-trivial. Firstly, we design a **Depth based Video data Generation** module **DVG** to handle the problem of data insufficiency. Similar to Wang et al. [64], DVG constructs a training pair of two views by utilizing forward-backward rendering, without the need of data annotation [49, 57, 68]. However, Wang et al. [64] only renders individual images, which will produce flickering results for video data generation [9]. In this paper, we improve the generation of video data for refining stereo occlusion masks by leveraging the inter-frame motion obtained from optical flow [28]. This methodology enables DVG to produce paired video data that maintains both geometric and temporal consistency. Leveraging paired video generated by DVG, we propose RefinerNet, along with a self-supervised video synthesis framework, to enable efficient and targeted training. More importantly, with access to sufficient paired videos, we devise a consistency control module, which consists of a metric of stereo deviation strength and a **Temporal Interaction Learning** module **TIL**. The stereo deviation strength aims to enable the generation of stereo videos in diverse real-world scenarios. A stereo-aware loss is further used to supervise the model in learning the magnitude of difference between the paired view features in the latent space. TIL integrates the latent features from long-temporal frames as a global information to augment the temporal coherence of the generated results.

Extensive experiments compared with various benchmark methods show that we achieve state-of-the-art performance. Notably, our SpatialDreamer meets the demand of real-world application without jitter, geometric and temporal inconsistency, which even beats AVP 3D converter and any open-source stereo video synthesis methods. We summarize our contributions as follows:

- A novel self-supervised stereo video synthesis framework, SpatialDreamer, is proposed, which is robust across a wide range of scenes and dynamic content in video. Moreover, equipping the DVG module, we build a stereo video dataset using a self-supervised approach.
- A consistency control module is devised, which consists of a metric of stereo deviation strength and a temporal interaction learning module, ensuring geometric and temporal consistency in video sequences.
- The sufficient experiments and quantitative results demonstrate that the proposed method outperforms the state-of-the-art methods, even beats AVP.

## 2. Related Work

### 2.1. Single-image Novel View Synthesis

Early studies address the single-image novel view synthesis task without relying on explicit 3D representation, such as End-to-end Synthesis [67], Infinite-Nature [35] and Animatable 3D Characters [66]. These methods do not utilize

explicit 3D representations for entire scenes, which limits the consistency of 3D views in the generated outputs and results in flickering and blurring, particularly in occluded regions. Layer-based methods, such as 3D-photography [54] and SLIDE [26] represent a 3D scene using discrete layers. Yet, the synthesized views may lack accuracy in texture and geometric consistency across different perspectives. SMPI [59], AdaMPI [21] and SinMPI [45] represent the 3D scene using multiple planes, while their rendered results may suffer from depth discretization artifacts and repetitive texture patterns. To reduce the reliance on large labeled datasets, Shi et.al [53], Wang et al. [64] and NVSVD-Net [4] explore self-supervised learning for creating novel view images from single image. Although they are capable of producing photorealistic results, they struggle to maintain temporal and spatial consistency, particularly in dynamic scenes.

As for our approach, we design a depth-based video generation module that generates paired videos with geometric and temporal priors. Additionally, Our method ensures multi-view consistency for the entire scene by employing a consistency control module.

### 2.2. Multi-view Novel View Synthesis

Early approaches in this field frequently utilized geometric methods, such as multi-view stereo reconstruction [29, 52] and structure-from-motion techniques [44, 51], to generate novel viewpoints from multiple images captured at different angles. NeRF-based methods were proposed to generate novel views based on fewer input images, including Sin-NeRF [70], CoPoNeRF [24] and NVIST [27]. 3D Gaussian Splatting [31] presented an explicit representation of the scene. Gaussian-based methods, such as pixelSplat [12] and MVsplat [14], can produce high-quality synthesis results from multi-view images. Recently, researchers have begun exploring the application of advanced diffusion models for novel view synthesis, driven by their remarkable success in this area. Notable approaches such as Photoconsistent-NVS [73], MultiDiff [40], GCD [61] and NVS-Solver [72] generate image sequences based on predefined camera trajectories using either single or multiple input images.

While these methods have shown promising results, they often suffer from limitations such as dependence on dense scene geometry, handling complex scene dynamics, and being hard to generalize [31]. Moreover, the challenge of optimizing NeRF/GS with a limited number of input views hampers the ability of multi-view NVS to produce high-quality results.

In contrast, we explore a video diffusion model to achieve stereo video synthesis, while preserving geometric structures through a RefinerNet based framework.

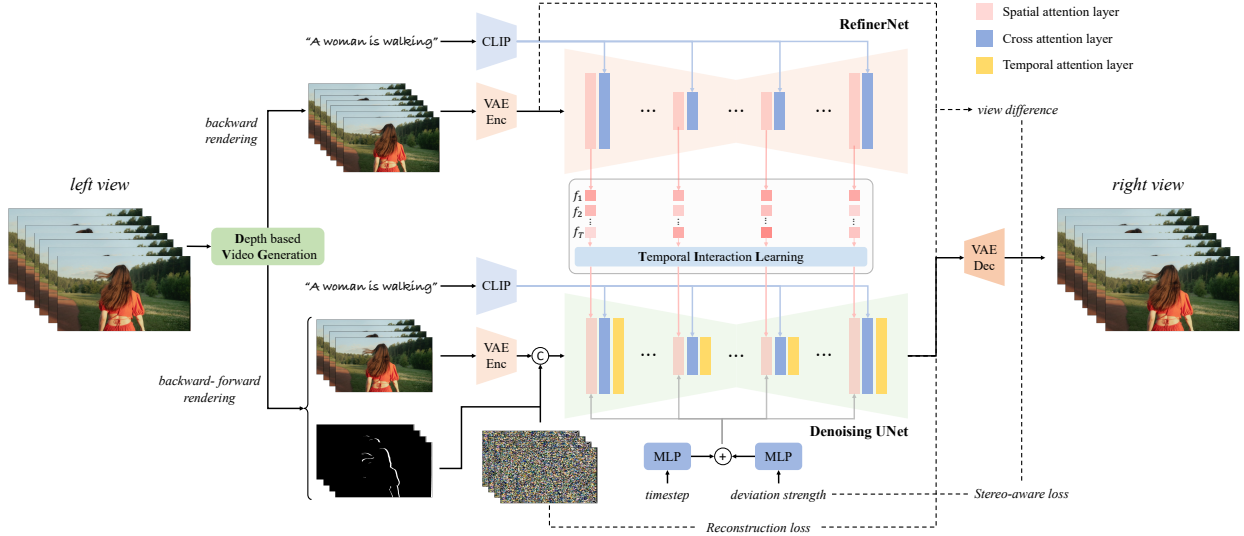


Figure 2. Overview of the proposed method, given left view video, the target view video is rendered, encoded, and concatenated with multi-frame noise, followed by the denoising U-Net architecture (i.e., SVD). The reference view images are fed into RefinerNet, through which the spatial features are extracted. **(Notably, the left and right views are the target and reference view respectively for training, and the opposite for inference).** The temporal interaction learning module integrates the latent features from long-temporal frames, and the deviation strength is projected as positional embedding and added to the time step embedding. Finally, the variational autoencoder decoder decodes the result into a video clip.

### 2.3. Video Synthesis via Diffusion Models

For video synthesis, previous works mainly expand image models to video, exploiting the image generation capability in the pretrained image diffusion models [36]. The video diffusion model (VDM) [23] and Video LDM [8] are proposed to adopt a 3D U-Net structure for joint image and video training. Subsequent works [15, 19, 19, 25, 55] also follow this insight with temporal attention, and [32, 46, 63, 69] further apply cross-frame attention to improve the consistency of the generated video. Another approach to promote temporal consistency is encoding video into 2D images [3, 43], which has been mainly explored in the video editing area. Although these models produce consistent results, they often require per-video optimization, which takes a long time, and would result in degradation when dealing with large motion. Most recently, [10, 20, 33] employ a transformer [62] architecture to model the temporal and spatial relations, demonstrating excellent video generation capabilities. However, these models need very large scale video datasets for training, which can be difficult to collect.

Beyond temporal information modeling, some works [13, 17, 65, 75] have introduced aligned spatial guidance to enhance the stability of the generated videos. The proposed framework also uses spatial guidance. Differing from those methods which require spatially aligned controls, a spatially unaligned reference image is used via a cross-attention mechanism. Furthermore, a metric of stereo deviation strength is introduced to strengthen the spatial constraint, resulting in more consistent results.

## 3. SpatialDreamer

Given an image sequence and a stereoscopic pose describing the scene depth information, the proposed method generates a stereo pair. In this section, we first provide a brief introduction about SVD [7]. Secondly, we offer detailed information of our proposed video generation module DVG, which can generate sufficient paired video with geometric and temporal consistency. Based on the DVG, we present the framework for self-supervised learning based video synthesis to support efficient and dedicate training. More importantly, to ensure the consistency between frames, we design a consistency control module for geometric and temporal consistency ensurance. Finally, we present the detailed training process.

### 3.1. Preliminaries

The challenge in video generation lies in accurately modeling the spatial-temporal dynamics, which involve understanding the spatial relationships within individual frames and the temporal relationships across frames. To address this challenge, Stable Video Diffusion (SVD) [7] introduces temporal convolution and attention layers. SVD follows the latent diffusion model (LDM) to encode video pixels into the latent space, enabling a more efficient denoising process. Given a video  $I_v$ , encoder  $\mathcal{E}$  encodes  $I_v$  into the latent space as  $z_0 = \mathcal{E}(I_v)$ . Gaussian noise  $\epsilon$  is then added in the Markov process:

$$z_t = \sqrt{\bar{\alpha}_t} z_0 + \sqrt{1 - \bar{\alpha}_t} \epsilon_t \quad (1)$$

where  $\bar{\alpha}_0, \dots, \bar{\alpha}_T$  are the pre-defined noise schedules for  $T$  steps in the Markov process. Notably, SVD is trained by the  $v$ -prediction formulation with the mean squared error (MSE) between the ground truth and its prediction in the latent space.

### 3.2. Depth based Video Generation

To create training pairs of images along with their corresponding occluded masks, the following self-supervised mechanism is employed utilizing real images. Firstly, the depth of the given video sample is estimated by MiDaS [47]. Secondly, the reference view image  $x_1$  is rendered into a masked one under the target viewpoint  $P_2$ , and then the trained inpainting model [56] is used to fill these occluded regions to obtain the novel viewpoint  $x_2$  [41]. Finally,  $x_2$  is rendered back to the original viewpoint  $P_1$  via a back rendering. After this, we can obtain the masked image  $\tilde{x}_1$  with mask  $M$  under viewpoint  $P_1$ , as well as the inpainted image  $x_2$  under viewpoint  $P_2$ . The mask  $M$  and masked image  $\tilde{x}_1$  are considered to be the conditions, with the image  $x_1$  serving as the ground truth for the diffusion model. This approach involves encoding the inpainted image  $x_2$  into latent feature representations and feeding it into RefinerNet.

However, the aforementioned approach encounters challenges in addressing inconsistencies among generated data frames, resulting in observable artifacts such as jittering and flickering. To tackle this issue, we leverage optical flow [58] to capture motion between successive video frames. Specifically, by leveraging the optical flow between the reference image  $x_1^t$  at time  $t$  and its adjacent frames, we establish the pixel correspondences between the image  $x_1^t$  and the images  $x_1^{t-1}$  and  $x_1^{t+1}$ , respectively. Particularly, these optical flows enable computing a confidence map via forward-backward consistency [16], which allows us to more accurately merge the stereo occlusions in the masks between adjacent frames [1]. Subsequently, the refined occlusion mask  $m^t$  is generated by sampling from the occlusion maps  $m^{t-1}$  and  $m^{t+1}$ , leveraging the pixel correspondences between consecutive frames under the reference view, as described by the following equation.

$$m^t(i, j) = \begin{cases} 1, & \sum_{k \in \{t-1, t+1\}} m^k(i + u, j + v) \cdot \\ & C(i, j) \geq 1 \\ m^t(i, j), & \text{else} \end{cases} \quad (2)$$

where  $u$  and  $v$  are the x and y components of the optical flow vector, and  $C$  represents the optical flow confidence measure. By propagating information from occluded areas across frames, this inter-frame continuity facilitates a more precise refinement of occluded regions in paired view

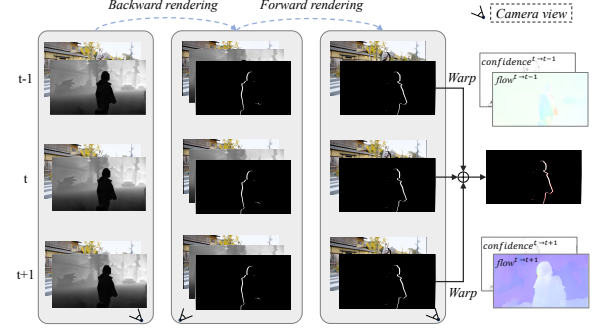


Figure 3. DVG. The temporal motion can be utilized to refine the occluded regions in the current frame, thereby providing smoother images and more consistent occlusion in the temporal sequence.

videos and enforces temporal smoothness and coherence within the self-supervised framework, effectively mitigating the undesirable effects of jitter and flicker.

As shown in Figure 3, the difference between the training and inference procedures is that the former uses both backward and forward rendering whereas the latter uses only forward rendering to obtain an image under the target view.

### 3.3. Self-Supervised Stereo Video Synthesis framework

Leveraging the generated paired view videos, we propose a self-supervised framework for stereo video synthesis, as illustrated in Fig 2. This framework commences with the rendering of the target view video that incorporates occlusions, followed by the application of a spatio-temporal method to effectively inpaint the missing regions, ultimately yielding a complete non-occluded target view video.

To learn the distribution of the feature space between the paired view images, we devise RefinerNet, which is modeled after the architecture of the denoising U-Net, excluding the temporal layer. RefinerNet adopts the weight initialization from the original SD2.1 model [48]. As depicted in Figure 2, a spatial attention layer is employed instead of the self-attention layer. Given a feature map  $z_t \in \mathbb{R}^{t \times h \times w \times c}$  from the denoising U-Net and another feature map  $z_r \in \mathbb{R}^{t \times h \times w \times c}$  from RefinerNet along with TIL module, they are concatenated along the  $h$  dimension, and then self-attention is applied. Subsequently, the first half of the feature map is retrieved as the output. One great advantage of this approach is that it enables RefinerNet to maintain the feature representation capability inherent in the original SD Unet, extracting reference view image information. In addition, the denoising U-Net can adaptively learn features from RefinerNet that are correlated in the same feature space, owing to the fundamentally similar network architectures between the denoising U-Net and RefinerNet. This not only ensures a robust initialization for the

feature representation but also enhances the learning ability of the entire network.

### 3.4. Consistency Control Module

#### 3.4.1 Temporal Interaction Learning module

While our RefinerNet-based approach providing spatial guidance, paired view features are still merged independently, posing challenges for temporal consistency and the generated images may exhibit discrepancies in texture or produce peculiar results, particularly between adjacent frames.

Inspired by previous studies [11, 22], we propose an attention-based temporal interaction learning module that learns the distribution of the feature space from adjacent frames, named TIL. Specifically, given latent codes of  $N_r$  adjacent images under reference view  $z_i^t$ , where  $i = 1, 2, \dots, N_r$  and the latent features of the reference view image  $z_r^t$  at the time step  $t$ , we augment the  $z_r^t$  to  $aug_r^t$  as:

$$aug_r^t = \lambda \cdot \text{Attn}_{r,r} + (1 - \lambda) \cdot \frac{1}{N_r} \sum_{i=1}^{N_r} \text{Attn}_{r,i} \quad (3)$$

where  $\lambda \in [0, 1]$  and  $\text{Attn}_{i,j}$  defines attention between two latent features  $z_i$  and  $z_j$ . This module blends the self-attention of  $z_r^t$  with the cross-view attention between  $z_r^t$  and each adjacent view  $z_i^t$ . The cross-view attention aligns the feature of all adjacent frames to the reference view while the self-attention helps each reference image retain distinctiveness.

The augmented reference feature  $aug_r^t$  is then fed into spatial attention layer to assist U-Net network learning.

#### 3.4.2 Stereo Deviation Strength

During the training, we noticed that different viewpoints impact the 3D impression of the scenes in the generated videos. However, relying solely on a given viewpoint as a guide for generating stereoscopic videos is insufficient. This is because videos with the same viewpoint may exhibit diverse depth ranges and variations, depending on the scene [68]. Therefore, pose alone cannot accurately control the 3D effect of a scene. Consequently, we introduce a metric called the stereo deviation strength, which quantitatively assesses the binocular disparity in a scene and facilitates the creation of controllable stereo vision:

$$s(z) = |z_0 - z_{ref}| \quad (4)$$

where the stereo deviation strength quantifies the latent differences between reference view  $z_{ref}$  and target view  $z_0$ . Similar to the time step, the deviation strength is projected into a positional embedding and added to each frame in the



Figure 4. Stereo deviation strength guidance examples. Augmenting the deviation strength enhances the 3D photography effect, but excessive deviation strength may lead to image distortions or even lower the quality of stereoscopic image.

residual block to ensure uniform application of the deviation strength to every frame. The impact of stereo deviation strength guidance on the results is illustrated in Figure 4.

Moreover, for better convergence, a stereo-aware loss function is proposed to directly supervise the disparity difference:

$$l_d = \|s(z_0) - s(\hat{z}_0)\|_2^2 \quad (5)$$

where  $\hat{z}_0$  represents the estimated clean video latent  $z_0$ , which can be obtained by:

$$\hat{z}_0 = z_0 - \frac{\sqrt{1 - \bar{\alpha}_t} \epsilon_\theta(z_t, c, t)}{\sqrt{\bar{\alpha}_t}} \quad (6)$$

where  $\bar{\alpha}_t = \prod_{i=1}^t (1 - \beta_t)$ , and the noise prediction loss is combined with the stereo-aware loss by a scaling factor:

$$l = l_\epsilon + \lambda \cdot l_d \quad (7)$$

### 3.5. Training Strategy

The training process is divided into two stages. In the first training stage, we focus on individual frames from videos. The temporal layer in denoising U-Net is frozen, and TIL module is removed. The RefinerNet model and the denoising U-Net are initialized with pretrained weights from SD2.1 [48] and SVD [7] respectively. The weights of the variational autoencoder encoder and decoder, as well as the contrastive language-image pre-training (CLIP) image encoder, are all kept fixed. The aim of this stage is for the model to learn to synthesize new viewpoint images under the condition of a reference image and a new viewpoint pose. In the second stage, we train the temporal layer and TIL module with video sequences. This enables the model to capture temporal context information efficiently. The input for the model is the 8-frame video clip and  $N_r$  for TIL is set to 8. During this stage, only the denoising U-Net and TIL module are trained while keeping the weights of the remaining network unchanged.

## 4. Experiments

### 4.1. Datasets, Baselines and Metrics

We conduct our experiments on image and video levels with RealEstate10K [76] and self-collected video data. RealEstate10K is a large, widely used dataset with camera poses, corresponding to 10 million frames derived from about 80,000 video clips, gathered from about 10,000 YouTube videos. As there is not open-source stereo video benchmark, we collect 1500 monocular videos with 1400 for training, 100 for testing. For the image synthesis, we compared the proposed method with recent open-source SOTA methods: 3D-photography [54], SynSin [67], AdaMPI [21], SinMPI [45], Wang et al. [64], Photoconsistent-NVS(P-NVS) [73], NVSVDE-Net [4], CoPoNeRF [24] and MVSplat [14]. For a fair comparison, the method of 3D-photography, AdaMPI, SinMPI, and the proposed method all used MiDaS [47] for the depth estimation. All the methods were conducted with the same intrinsic matrices, source camera poses, and target camera poses. Following the method of 3D-photography [54], we measured the accuracy of the generated target views with regard to the ground-truth images using the three metrics of the learned perceptual image patch similarity (LPIPS), peak signal-to-noise ratio (PSNR), and structural similarity index measure (SSIM).

For the video synthesis, we picked several representative approaches, i.e., the method of 3D-photography [54], the open-source code repository webui-depthmap<sup>1</sup>, P-NVS [73], CoPoNeRF [24], NVS-Solver [72] and AVP [42]. Moreover, we conducted the same depth estimation method [47] for a fair comparison of 3D-photography [54], webui-depthmap and NVS-Solver [72]. We employ the FVD [60] score to measure the perceptual similarity between input videos and outputs and report the flow warping error  $E_{warp}$  [34] to assess the temporal consistency of the resulting video sequences.

### 4.2. Implementation

We employed the AdamW [37] optimizer with a learning rate of  $1 \times 10^{-5}$  for training the model. All the experiments were conducted using two NVIDIA A800 GPUs. In the first training stage, individual video frames were sampled, resized, and center-cropped to a resolution of  $1024 \times 1024$ . We trained the model for 100,000 iterations with a batch size of 8. In the second training stage, the videos were first split according to the transitions to ensure that a scene only appeared in one video clip. We then formed each video clip for training with eight frames. Finally, the temporal layer and TIL module was trained for 10,000 steps with a batch size of 2. The stereo-aware loss scaling factor  $\lambda$  was set to 0.001 and  $\lambda$  in Eq. 3 was set as 0.6.

<sup>1</sup><https://github.com/thygate/stable-diffusion-webui-depthmap-script>

	SSIM $\uparrow$		PSNR $\uparrow$		LPIPS $\downarrow$	
	$t=5$	$t=10$	$t=5$	$t=10$	$t=5$	$t=10$
3D-photography [54] $\dagger$	0.641	0.446	11.08	9.533	0.116	0.386
SynSin [67] $\dagger$	0.740	0.645	21.22	19.55	0.087	0.104
AdaMPI [21] $\dagger$	0.869	0.736	27.70	22.65	0.041	0.087
SinMPI [45] $\dagger$	0.898	0.775	28.79	23.21	0.040	0.080
Wang et al. [64]	0.840	0.720	25.35	21.36	0.049	0.095
P-NVS [73] $\dagger$	0.724	0.667	21.98	19.46	0.241	0.279
NVSVDE-Net [4]		0.840		24.31		0.233
CoPoNeRF [24] $\dagger$	0.658	0.632	22.63	21.33	0.171	0.209
MVSplat [14] $\dagger$		0.863		25.89		0.132
Proposed	<b>0.916</b>	<b>0.857</b>	<b>32.26</b>	<b>24.86</b>	<b>0.038</b>	<b>0.049</b>

Table 1. Quantitative comparison on RealEstate10K dataset.  $\dagger$  means re-implementing in our setting for fair comparison. The best results are in **bold**.

### 4.3. Qualitative Results

#### 4.3.1 Stereo Image Synthesis

We visually compared the outputs of the different methods by generating a new view image given the target viewpoint. We qualitatively compare the newly synthesized images in Figure 5. 3D-photography fails to resolve the image distortion problem, and the image appears to be enhanced only slightly by the rendering. SynSin generates the most blurry details and loses a lot of information, compared with the input view. Neither AdaMPI nor SinMPI can generate fine enough details, and the results contain noticeable artifacts. CoPoNeRF tends to produce discrepancies from the original image in terms of fine-grained details, and it struggles with effectively handling scenes involving motion, as well as MVSplat. In contrast, the proposed method shows a clean and detailed output, especially in the area of depth information discontinuity.

#### 4.3.2 Stereo Video Synthesis

Moreover, we qualitatively compared the results of the stereo video synthesis with other methods. In addition to the quality issues of single-frame generation, the most important aspect in videos is the temporal consistency. We seek to generate videos that are free of flicker. The visualization of generated videos from different methods are illustrated in Figure 6, for each video, we show the scanline (the yellow line in figure) slice through the spatial-temporal volume. Our method achieve the smoothest trajectories, while other methods exhibit significant flickering. The most distinct regions are zoomed in and highlighted under the images to illustrate the details. In the first case, our method maintain the texture of the trees behind the woman. And the second case, only our method attain the smooth trajec-

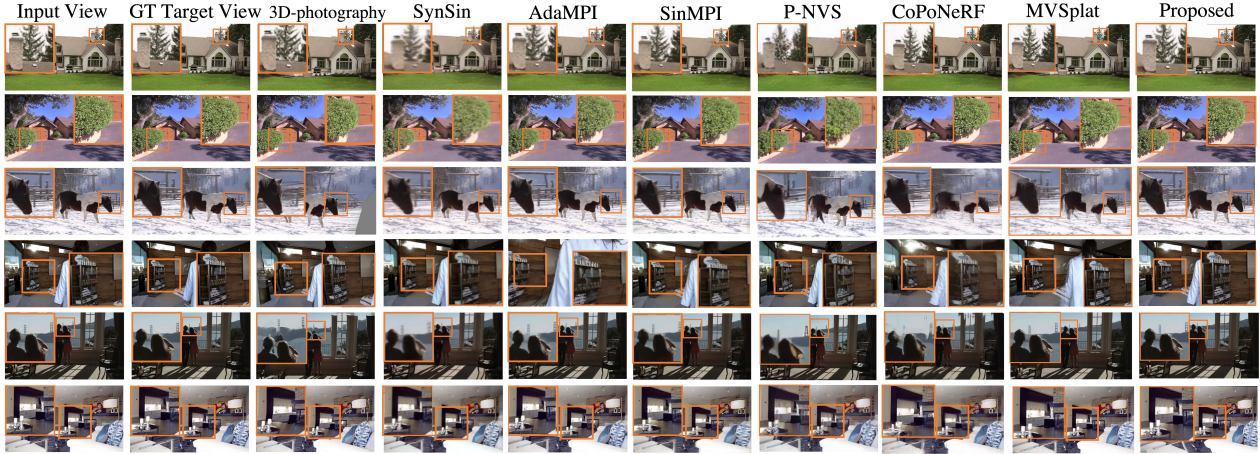


Figure 5. Qualitative results on the RealEstate10K dataset. The proposed method generates better-quality information and maintains the edge and textural details of the reference image better than the other methods. More results are available in supplementary material.



Figure 6. Visual comparisons in stereo video benchmark. We show the scanline (yellow line in original frame) slice through the spatial-temporal volume. The most distinct regions are zoomed in and highlighted under the images to illustrate the details.

	FVD $\downarrow$	$E_{warp}^* \downarrow$
3D-photography [54]	155.0	3.418
Webui-depthmap	83.18	3.486
P-NVS [73]	420.2	23.02
CoPoNeRF [24]	290.0	7.144
NVS-Solver [72]	249.1	5.842
AVP [42]	99.92	3.446
<b>Proposed</b>	<b>67.09</b>	<b>3.374</b>

Table 2. Quantitative comparison with the other methods. The best results are in **bold**.  $E_{warp}^*$  denotes  $E_{warp}$  ( $\times 10^{-3}$ ).

ries of the background (maintaining the straight line). And the last case, only our method maintain the texture of the black vertical lines. More results of generated frames are also presented in supplementary material.

#### 4.4. Quantitative Results

Table 1 lists the SSIM, PSNR, and LPIPS scores for the newly synthesized images. The proposed method outperforms 3D-photography and SynSin in the major metrics by a wide margin. The method of Wang et al., CoPoNeRF and P-NVS perform slightly worse in terms of all metrics compared to the proposed method. Since the proposed method merges the spatial features and fills the occluded regions, it achieves the best LPIPS scores and shows competitive results in PSNR and SSIM when compared with AdaMPI and MVsplat. Overall, the results exhibit superior visual effects, which is consistent with the performance observed in the qualitative experiments. We further demonstrate the effectiveness of our method on video synthesis, the results are shown in Table 2. The proposed method achieves the best performance on both FVD and  $E_{warp}$ , which means our generated videos attain the best quality and temporal consistency.

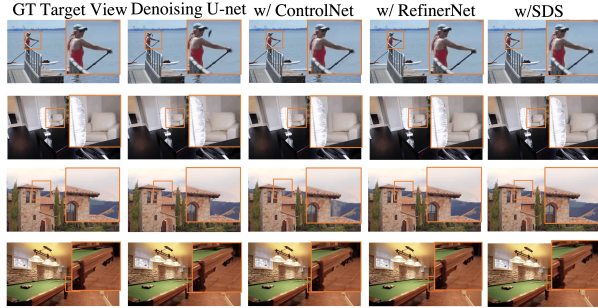


Figure 7. Ablation study of different designs. Only the proposed method ensures consistent preservation of details with the ground-truth target view. More results are available in supplementary material.

Method	CN RN SDS TIL DVG				Stereo Image			Stereo Video	
	SSIM↑	PSNR↑	LPIPS↓	FVD↓					
Image-level	✓				0.880	23.73	0.06	-	
		✓			0.855	24.04	0.183	-	
			✓		0.895	30.20	0.043	-	
			✓	✓	<b>0.916</b>	<b>32.26</b>	<b>0.038</b>	-	
Video-level	✓	✓			-	-	-	184.0	
	✓	✓	✓		-	-	-	123.5	
	✓	✓	✓	✓	-	-	-	85.21	
	✓	✓	✓	✓	-	-	-	<b>67.09</b>	

Table 3. Quantitative comparison for the ablation study. The best results are in **bold**.

## 4.5. Ablation Study

### 4.5.1 Effectiveness of each components

We show the results in Table 3 on the RealEstate10K (stereo image) and collected stereo video datasets. CN means substituting our RefinerNet (RN) to ControlNet, SDS means the proposed stereo deviation strength. **For image-level comparison**, the results show that utilizing U-Net architecture only is not sufficient for stereo image synthesis and our RefinerNet is a better choice than ControlNet. Adding SDS further improves the geometric consistency. As visualized in Fig 7, solely relying on U-Net features results in distortion in the edge area and struggles with generating content properly. It also fails to preserve textural details near a plane boundary. Adding ControlNet often results in content inconsistency, presumably due to the failure of the paired view feature integration. RefinerNet handles this problem, showing it is a better architecture for stereo image generation. SDS further improves the consistency with the input and contain a more detailed image structure. As for **video-level comparison**, the quantitative results are shown in Table 3, adding TIL and DVG both attain the performance gain, and our final model achieves the best performance.



Figure 8. Visual comparisons for the improvement of stereo occlusion. We show the scanline of (yellow line in original frame) slice through the spatial-temporal volume. The red region represents the changes of occlusion mask.

### 4.5.2 Data improvement by DVG

We show the generated stereo occlusion mask with inter-frame motion refinement in Fig 8. It can be observed that the occlusions appear more complete spatially and exhibit smoother in their temporal distribution. By employing DVG, we can acquire sufficient data to support the generation of spatio-temporally consistent videos.

### 4.5.3 Exploration of different depth estimation methods

We further compare different design choices of depth map including DepthAnything [71], Marigold [30], MiDaS [47] and ZoeDepth [5]. The results are available in supplementary materials. The proposed method can produce new viewpoint images that are realistic, seamless, and rich in detail, regardless of the depth estimation method used. This capability demonstrates the versatility and robustness of the proposed method, ensuring superior performance in various applications and environments.

## 5. Conclusion

In this paper, we introduce a new self-supervised stereo video synthesis approach using a video diffusion model, termed SpatialDreamer. This method addresses the issues of insufficient data and spatio-temporal inconsistency between frames. To solve the problem of insufficient data, we develop a Depth-based Video Generation (DVG) module that uses a forward-backward rendering mechanism to generate a rendered video with geometric and temporal priors. Additionally, we propose RefinerNet along with a self-supervised synthetic framework to enable efficient and dedicated training using data generated by DVG. Furthermore, we design a consistency control module to ensure geometric and temporal consistency. Our SpatialDreamer outperforms all other open-source stereo image and video synthesis methods and has the potential for future expansion into virtual reality applications.

## References

[1] Dmitry Akimov, Alexey Shestov, Alexander Voronov, and Dmitriy Vatolin. Occlusion refinement for stereo video using optical flow. In *2012 International Conference on 3D Imaging (IC3D)*, pages 1–8, 2012. 4

[2] Andrea Schubert. visionos 2 brings new spatial computing experiences to apple vision pro. <https://www.apple.com/newsroom/2024/06/visionos-2-brings-new-spatial-computing-experiences-to-apple-vision-pro>, 2024. 1

[3] Omer Bar-Tal, Dolev Ofri-Amar, Rafail Fridman, Yoni Kassten, and Tali Dekel. Text2live: Text-driven layered image and video editing. In *European conference on computer vision*, pages 707–723. Springer, 2022. 3

[4] Juan Luis Gonzalez Bello and Munchurl Kim. Novel view synthesis with view-dependent effects from a single image. In *Proceedings of the IEEE/CVF Conference on Computer Vision and Pattern Recognition*, 2024. 2, 6

[5] Shariq Farooq Bhat, Reiner Birkl, Diana Wofk, Peter Wonka, and Matthias Müller. Zoedepth: Zero-shot transfer by combining relative and metric depth, 2023. 8

[6] Phuong Ngoc Binh Do and Quoc Chi Nguyen. A review of stereo-photogrammetry method for 3-d reconstruction in computer vision. In *2019 19th International Symposium on Communications and Information Technologies (ISCIT)*, pages 138–143, 2019. 1

[7] Andreas Blattmann, Tim Dockhorn, Sumith Kulal, Daniel Mendelevitch, Maciej Kilian, Dominik Lorenz, Yam Levi, Zion English, Vikram Voleti, Adam Letts, et al. Stable video diffusion: Scaling latent video diffusion models to large datasets. *arXiv preprint arXiv:2311.15127*, 2023. 3, 5

[8] Andreas Blattmann, Robin Rombach, Huan Ling, Tim Dockhorn, Seung Wook Kim, Sanja Fidler, and Karsten Kreis. Align your latents: High-resolution video synthesis with latent diffusion models. In *Proceedings of the IEEE/CVF Conference on Computer Vision and Pattern Recognition*, pages 22563–22575, 2023. 3

[9] Aaron Bobick and Stephen Intille. Large occlusion stereo. *International Journal of Computer Vision*, 33:181–200, 1999. 2

[10] Tim Brooks, Bill Peebles, Connor Holmes, Will DePue, Yufei Guo, Li Jing, David Schnurr, Joe Taylor, Troy Luhman, Eric Luhman, Clarence Ng, Ricky Wang, and Aditya Ramesh. Video generation models as world simulators. 2024. 3

[11] Mingdeng Cao, Xintao Wang, Zhongang Qi, Ying Shan, Xiaohu Qie, and Yinqiang Zheng. Masactrl: Tuning-free mutual self-attention control for consistent image synthesis and editing, 2023. 5

[12] David Charatan, Sizhe Li, Andrea Tagliasacchi, and Vincent Sitzmann. pixelsplat: 3d gaussian splats from image pairs for scalable generalizable 3d reconstruction. In *arXiv*, 2023. 2

[13] Weifeng Chen, Jie Wu, Pan Xie, Hefeng Wu, Jiashi Li, Xin Xia, Xuefeng Xiao, and Liang Lin. Control-a-video: Controllable text-to-video generation with diffusion models. *arXiv preprint arXiv:2305.13840*, 2023. 3

[14] Yuedong Chen, Haofei Xu, Chuanxia Zheng, Bohan Zhuang, Marc Pollefeys, Andreas Geiger, Tat-Jen Cham, and Jianfei Cai. Mvsplat: Efficient 3d gaussian splatting from sparse multi-view images. *arXiv preprint arXiv:2403.14627*, 2024. 2, 6

[15] Zuozhuo Dai, Zhenghao Zhang, Yao Yao, Bingxue Qiu, Siyu Zhu, Long Qin, and Weizhi Wang. Animateanything: Fine-grained open domain image animation with motion guidance. *arXiv e-prints*, pages arXiv–2311, 2023. 3

[16] G. Egnal and R.P. Wildes. Detecting binocular half-occlusions: empirical comparisons of five approaches. *IEEE Transactions on Pattern Analysis and Machine Intelligence*, 24(8):1127–1133, 2002. 4

[17] Patrick Esser, Johnathan Chiu, Parmida Atighehchian, Jonathan Granskog, and Anastasis Germanidis. Structure and content-guided video synthesis with diffusion models. In *Proceedings of the IEEE/CVF International Conference on Computer Vision*, pages 7346–7356, 2023. 3

[18] Chen Gao, Ayush Saraf, Johannes Kopf, and Jia-Bin Huang. Dynamic view synthesis from dynamic monocular video, 2021. 1

[19] Yuwei Guo, Ceyuan Yang, Anyi Rao, Zhengyang Liang, Yaohui Wang, Yu Qiao, Maneesh Agrawala, Dahua Lin, and Bo Dai. Animatediff: Animate your personalized text-to-image diffusion models without specific tuning. *International Conference on Learning Representations*, 2024. 3

[20] Agrim Gupta, Lijun Yu, Kihyuk Sohn, Xiuye Gu, Meera Hahn, Li Fei-Fei, Irfan Essa, Lu Jiang, and José Lezama. Photorealistic video generation with diffusion models. *arXiv preprint arXiv:2312.06662*, 2023. 3

[21] Yuxuan Han, Ruicheng Wang, and Jiaolong Yang. Single-view view synthesis in the wild with learned adaptive multiplane images. In *ACM SIGGRAPH 2022 Conference Proceedings*, pages 1–8, 2022. 1, 2, 6

[22] Amir Hertz, Ron Mokady, Jay Tenenbaum, Kfir Aberman, Yael Pritch, and Daniel Cohen-Or. Prompt-to-prompt image editing with cross attention control, 2022. 5

[23] Jonathan Ho, Tim Salimans, Alexey Gritsenko, William Chan, Mohammad Norouzi, and David J Fleet. Video diffusion models. In *Advances in Neural Information Processing Systems*. Curran Associates, Inc., 2022. 3

[24] Sunghwan Hong, Jaewoo Jung, Heesong Shin, Jiaolong Yang, Seungryong Kim, and Chong Luo. Unifying correspondence, pose and nerf for pose-free novel view synthesis from stereo pairs, 2024. 2, 6, 7

[25] Li Hu, Xin Gao, Peng Zhang, Ke Sun, Bang Zhang, and Liefeng Bo. Animate anyone: Consistent and controllable image-to-video synthesis for character animation. *arXiv preprint arXiv:2311.17117*, 2023. 3

[26] Varun Jampani, Huiwen Chang, Kyle Sargent, Abhishek Kar, Richard Tucker, Michael Krainin, Dominik Kaeser, William T Freeman, David Salesin, Brian Curless, et al. Slide: Single image 3d photography with soft layering and depth-aware inpainting. In *Proceedings of the IEEE/CVF International Conference on Computer Vision*, pages 12518–12527, 2021. 2

[27] Wonbong Jang and Lourdes Agapito. Nvist: In the wild new view synthesis from a single image with transformers, 2024. 2

[28] Jisoo Jeong, Hong Cai, Risheek Garrepalli, Jamie Menjaj Lin, Munawar Hayat, and Fatih Porikli. Ocai: Improving optical flow estimation by occlusion and consistency aware interpolation, 2024. 2

[29] Hailin Jin, Stefano Soatto, and Anthony J Yezzi. Multi-view stereo reconstruction of dense shape and complex appearance. *International Journal of Computer Vision*, 63:175–189, 2005. 2

[30] Bingxin Ke, Anton Obukhov, Shengyu Huang, Nando Metzger, Rodrigo Caye Daudt, and Konrad Schindler. Repurposing diffusion-based image generators for monocular depth estimation, 2024. 8

[31] Bernhard Kerbl, Georgios Kopanas, Thomas Leimkühler, and George Drettakis. 3d gaussian splatting for real-time radiance field rendering, 2023. 1, 2

[32] Levon Khachatryan, Andranik Mousisyan, Vahram Tadevosyan, Roberto Henschel, Zhangyang Wang, Shant Navasardyan, and Humphrey Shi. Text2video-zero: Text-to-image diffusion models are zero-shot video generators. *arXiv preprint arXiv:2303.13439*, 2023. 3

[33] Dan Kondratyuk, Lijun Yu, Xiuye Gu, José Lezama, Jonathan Huang, Rachel Hornung, Hartwig Adam, Hassan Akbari, Yair Alon, Vighnesh Birodkar, et al. Videopoet: A large language model for zero-shot video generation. *arXiv preprint arXiv:2312.14125*, 2023. 3

[34] Wei-Sheng Lai, Jia-Bin Huang, Oliver Wang, Eli Shechtman, Ersin Yumer, and Ming-Hsuan Yang. Learning blind video temporal consistency. In *Proceedings of the European conference on computer vision (ECCV)*, pages 170–185, 2018. 6

[35] Andrew Liu, Richard Tucker, Varun Jampani, Ameesh Makadia, Noah Snavely, and Angjoo Kanazawa. Infinite nature: Perpetual view generation of natural scenes from a single image. In *Proceedings of the IEEE/CVF International Conference on Computer Vision*, 2021. 2

[36] Yixin Liu, Kai Zhang, Yuan Li, Zhiling Yan, Chujie Gao, Ruoxi Chen, Zhengqing Yuan, Yue Huang, Hanchi Sun, Jianfeng Gao, Lifang He, and Lichao Sun. Sora: A review on background, technology, limitations, and opportunities of large vision models, 2024. 3

[37] Ilya Loshchilov and Frank Hutter. Decoupled weight decay regularization. *arXiv preprint arXiv:1711.05101*, 2017. 6

[38] Kevin Matzen, Michael F. Cohen, Bryce Evans, Johannes Kopf, and Richard Szeliski. Low-cost 360 stereo photography and video capture. *ACM Trans. Graph.*, 36(4), 2017. 1

[39] Ben Mildenhall, Pratul P. Srinivasan, Matthew Tancik, Jonathan T. Barron, Ravi Ramamoorthi, and Ren Ng. Nerf: Representing scenes as neural radiance fields for view synthesis, 2020. 1

[40] Norman Müller, Katja Schwarz, Barbara Rössle, Lorenzo Porzi, Samuel Rota Bulò, Matthias Nießner, and Peter Kontschieder. Multidiff: Consistent novel view synthesis from a single image. In *Proceedings of the IEEE/CVF Conference on Computer Vision and Pattern Recognition*, pages 10258–10268, 2024. 2

[41] Simon Niklaus and Feng Liu. Softmax splatting for video frame interpolation, 2020. 4

[42] Onee. What is spatial video on iphone 15 pro and vision pro. <https://xreality.zone/en/posts/what-is-spatial-video-on-iphone-15-pro-and-apple-vision-pro>, 2024. 1, 6, 7

[43] Hao Ouyang, Qiuyu Wang, Yuxi Xiao, Qingyan Bai, Juntao Zhang, Kecheng Zheng, Xiaowei Zhou, Qifeng Chen, and Yujun Shen. Codef: Content deformation fields for temporally consistent video processing. *arXiv preprint arXiv:2308.07926*, 2023. 3

[44] Onur Özyeşil, Vladislav Voroninski, Ronen Basri, and Amit Singer. A survey of structure from motion\*. *Acta Numerica*, 26:305–364, 2017. 2

[45] Guo Pu, Peng-Shuai Wang, and Zhouhui Lian. Sinmp: Novel view synthesis from a single image with expanded multiplane images, 2023. 2, 6

[46] Chenyang Qi, Xiaodong Cun, Yong Zhang, Chenyang Lei, Xintao Wang, Ying Shan, and Qifeng Chen. Fatezero: Fusing attentions for zero-shot text-based video editing. *arXiv preprint arXiv:2303.09535*, 2023. 3

[47] René Ranftl, Katrin Lasinger, David Hafner, Konrad Schindler, and Vladlen Koltun. Towards robust monocular depth estimation: Mixing datasets for zero-shot cross-dataset transfer. *IEEE Transactions on Pattern Analysis and Machine Intelligence*, 44(3), 2022. 4, 6, 8

[48] Robin Rombach, Andreas Blattmann, Dominik Lorenz, Patrick Esser, and Björn Ommer. High-resolution image synthesis with latent diffusion models. In *Proceedings of the IEEE/CVF conference on computer vision and pattern recognition*, pages 10684–10695, 2022. 1, 4, 5

[49] Christoph Sager, Christian Janiesch, and Patrick Zschech. A survey of image labelling for computer vision applications. *Journal of Business Analytics*, 4(2):91–110, 2021. 2

[50] D. Scharstein. *View Synthesis Using Stereo Vision*. Springer Berlin Heidelberg, 1999. 1

[51] Johannes L Schonberger and Jan-Michael Frahm. Structure-from-motion revisited. In *Proceedings of the IEEE conference on computer vision and pattern recognition*, pages 4104–4113, 2016. 2

[52] S.M. Seitz, B. Curless, J. Diebel, D. Scharstein, and R. Szeliski. A comparison and evaluation of multi-view stereo reconstruction algorithms. In *2006 IEEE Computer Society Conference on Computer Vision and Pattern Recognition (CVPR'06)*, pages 519–528, 2006. 2

[53] Yujiao Shi, Hongdong Li, and Xin Yu. Self-supervised visibility learning for novel view synthesis.\*. In *Proceedings of the IEEE Conference on Computer Vision and Pattern Recognition*, 2021. 2

[54] Meng-Li Shih, Shih-Yang Su, Johannes Kopf, and Jia-Bin Huang. 3d photography using context-aware layered depth inpainting. In *Proceedings of the IEEE/CVF Conference on Computer Vision and Pattern Recognition*, pages 8028–8038, 2020. 2, 6, 7

[55] Uriel Singer, Adam Polyak, Thomas Hayes, Xi Yin, Jie An, Songyang Zhang, Qiyuan Hu, Harry Yang, Oron Ashual, Oran Gafni, et al. Make-a-video: Text-to-video generation without text-video data. *arXiv preprint arXiv:2209.14792*, 2022. 3

[56] Lorenzo Stacchio. Train stable diffusion for inpainting, 2023. 4

[57] Wenxiu Sun, Lingfeng Xu, Oscar C Au, Sung Him Chui, and Chun Wing Kwok. An overview of free view-point depth-image-based rendering (dibr). In *APSIPA Annual Summit and Conference*, pages 1023–1030, 2010. 1, 2

[58] Zachary Teed and Jia Deng. Raft: Recurrent all-pairs field transforms for optical flow, 2020. 4

[59] Richard Tucker and Noah Snavely. Single-view view synthesis with multiplane images. In *Proceedings of the IEEE/CVF Conference on Computer Vision and Pattern Recognition*, pages 551–560, 2020. 2

[60] Thomas Unterthiner, Sjoerd van Steenkiste, Karol Kurach, Raphaël Marinier, Marcin Michalski, and Sylvain Gelly. FVD: A new metric for video generation. In *Deep Generative Models for Highly Structured Data, ICLR 2019 Workshop, New Orleans, Louisiana, United States, May 6, 2019. OpenReview.net*, 2019. 6

[61] Basile Van Hoorick, Rundi Wu, Ege Ozguroglu, Kyle Sargent, Ruoshi Liu, Pavel Tokmakov, Achal Dave, Changxi Zheng, and Carl Vondrick. Generative camera dolly: Extreme monocular dynamic novel view synthesis. *European Conference on Computer Vision (ECCV)*, 2024. 2

[62] Ashish Vaswani, Noam Shazeer, Niki Parmar, Jakob Uszkoreit, Llion Jones, Aidan N Gomez, Łukasz Kaiser, and Illia Polosukhin. Attention is all you need. *Advances in neural information processing systems*, 30, 2017. 3

[63] Wen Wang, Yan Jiang, Kangyang Xie, Zide Liu, Hao Chen, Yue Cao, Xinlong Wang, and Chunhua Shen. Zero-shot video editing using off-the-shelf image diffusion models. *arXiv preprint arXiv:2303.17599*, 2023. 3

[64] Xiaodong Wang, Chenfei Wu, Shengming Yin, Minheng Ni, Jianfeng Wang, Linjie Li, Zhengyuan Yang, Fan Yang, Li-juan Wang, Zicheng Liu, et al. Learning 3d photography videos via self-supervised diffusion on single images. *arXiv preprint arXiv:2302.10781*, 2023. 1, 2, 6

[65] Xiang Wang, Hangjie Yuan, Shiwei Zhang, Dayou Chen, Jiumiu Wang, Yingya Zhang, Yujun Shen, Deli Zhao, and Jingen Zhou. Videocomposer: Compositional video synthesis with motion controllability. *Advances in Neural Information Processing Systems*, 36, 2024. 1, 3

[66] Chung-Yi Weng, Brian Curless, and Ira Kemelmacher-Shlizerman. Photo wake-up: 3d character animation from a single photo. In *Proceedings of the IEEE/CVF conference on computer vision and pattern recognition*, pages 5908–5917, 2019. 2

[67] Olivia Wiles, Georgia Gkioxari, Richard Szeliski, and Justin Johnson. Synsin: End-to-end view synthesis from a single image. In *Proceedings of the IEEE/CVF Conference on Computer Vision and Pattern Recognition*, 2020. 2, 6

[68] Andrew Woods, Tom Docherty, and Rolf Koch. Image distortions in stereoscopic video systems. *Proc SPIE*, 1915, 2002. 1, 2, 5

[69] Jay Zhangjie Wu, Yixiao Ge, Xintao Wang, Stan Weixian Lei, Yuchao Gu, Yufei Shi, Wynne Hsu, Ying Shan, Xiaohu Qie, and Mike Zheng Shou. Tune-a-video: One-shot tuning of image diffusion models for text-to-video generation. In *Proceedings of the IEEE/CVF International Conference on Computer Vision*, pages 7623–7633, 2023. 3

[70] Dejia Xu, Yifan Jiang, Peihao Wang, Zhiwen Fan, Humphrey Shi, and Zhangyang Wang. Sinnerf: Training neural radiance fields on complex scenes from a single image, 2022. 2

[71] Lihe Yang, Bingyi Kang, Zilong Huang, Xiaogang Xu, Jiashi Feng, and Hengshuang Zhao. Depth anything: Unleashing the power of large-scale unlabeled data, 2024. 8

[72] Meng You, Zhiyu Zhu, Hui Liu, and Junhui Hou. Nvs-solver: Video diffusion model as zero-shot novel view synthesizer. *arXiv preprint arXiv:2405.15364*, 2024. 2, 6, 7

[73] Jason J. Yu, Fereshteh Forghani, Konstantinos G. Derpanis, and Marcus A. Brubaker. Long-term photometric consistent novel view synthesis with diffusion models, 2023. 2, 6, 7

[74] Guofeng Zhang, Wei Hua, Xueying Qin, Tien-Tsin Wong, and Hujun Bao. Stereoscopic video synthesis from a monocular video. *IEEE Transactions on Visualization and Computer Graphics*, 13(4):686–696, 2007. 1

[75] Min Zhao, Rongzhen Wang, Fan Bao, Chongxuan Li, and Jun Zhu. Controlvideo: Adding conditional control for one shot text-to-video editing. *arXiv preprint arXiv:2305.17098*, 2023. 3

[76] Tinghui Zhou, Richard Tucker, John Flynn, Graham Fyffe, and Noah Snavely. Stereo magnification: Learning view synthesis using multiplane images. *CoRR*, abs/1805.09817, 2018. 6